Biochimica et Biophysica Acta 1798 (2010) 861–871

Contents lists available at ScienceDirect

Biochimica et Biophysica Acta

journal homepage: www.elsevier.com/locate/bbamem

Interaction of the exported malaria protein Pf332 with the red blood cell membrane skeleton

Karena L. Waller [a], Lisa M. Stubberfield [a], Valentina Dubljevic [a], Donna W. Buckingham [a], Narla Mohandas [c], Ross L. Coppel [a,b,1], Brian M. Cooke [a,*,1]

[a] Department of Microbiology, Monash University, VIC 3800, Australia
[b] Victorian Bioinformatics Consortium, Monash University, VIC 3800, Australia
[c] New York Blood Centre, New York NY 10021, USA

ARTICLE INFO

Article history:
Received 29 May 2009
Received in revised form 14 January 2010
Accepted 25 January 2010
Available online 2 February 2010

Keywords:
Plasmodium falciparum
Malaria
Pf332
Actin
Red blood cell
Membrane skeleton

ABSTRACT

Intra-erythrocytic *Plasmodium falciparum* malaria parasites synthesize and export numerous proteins into the red blood cell (RBC) cytosol, where some bind to the RBC membrane skeleton. These interactions are responsible for the altered antigenic, morphological and functional properties of parasite-infected red blood cells (IRBCs). *Plasmodium falciparum* protein 332 (Pf332) is a large parasite protein that associates with the membrane skeleton and who's function has recently been elucidated. Using recombinant fragments of Pf332 in *in vitro* interaction assays, we have localised the specific domain within Pf332 that binds to the RBC membrane skeleton to an 86 residue sequence proximal to the C-terminus of Pf332. We have shown that this region partakes in a specific and saturable interaction with actin ($K_d = 0.60\ \mu M$) but has no detectable affinity for spectrin. The only exported malaria protein previously known to bind to actin is PfEMP3 but here we demonstrate that there is no competition for actin-binding between PfEMP3 and Pf332, suggesting that they bind to different target sequences in actin.

1. Introduction

Malaria is the most important parasitic disease of humans, each year causing more than one million deaths predominantly in young children [1]. Malaria's severe pathophysiology results from the development of *Plasmodium* spp. parasites inside red blood cells (RBCs). Compared to normal human RBCs, parasite-infected RBCs (IRBCs) exhibit markedly altered morphological, antigenic and functional properties, including increased membrane rigidity, reduced RBC deformability, the appearance of electron dense knobs on the RBC membrane surface and the ability to adhere to vascular endothelium (see Cooke et al., for review [2]). These parasite-induced modifications result from the synthesis and export of numerous parasite-encoded proteins from the intracellular parasite into the RBC cytosol. Some of these exported proteins participate in protein interactions with RBC membrane skeleton proteins, affecting the structural and mechanical integrity of the IRBC, and in some cases, are major contributors to falciparum malaria's unique virulence (see Cooke et al., for review [2]).

The membrane skeleton of a normal human RBC consists of a regular array of numerous proteins, with the major structural components being αβ-spectrin heterodimers, actin and protein 4.1 (4.1R). Actin is a 43 kDa monomer protein that oligomerises to form 30–40 nm long filaments containing 12–14 monomer units which are predominantly located at the vertices of the spectrin hexagonal array in regions known as junctional complexes (see Walensky et al., for review [3]). Actin participates in interactions with both spectrin and 4.1R, forming the spectrin–actin–4.1R ternary complex and the structural backbone of the membrane skeleton. In this ternary complex, 4.1R functions to stabilise the spectrin–actin interactions (see Gascard and Mohandas [4] for review). To date, mapping studies have defined a 140 residue region located in the N-terminal region of β-spectrin and a 26 residue region in 4.1R that bind actin [5,6], however the residues in actin that bind spectrin and 4.1R are not yet delineated. Additional protein interactions between 4.1R, the transmembrane proteins glycophorins C and D (GPC and GPD,

Abbreviations: RBC, red blood cell; IRBC, infected red blood cell; Pf332 or Ag332, *Plasmodium falciparum* Antigen 332; K_d, half saturation concentration; 4.1R, red blood cell protein 4.1; GPC and GPD, glycophorins C and D, respectively; PfEMP1, *Plasmodium falciparum* erythrocyte membrane protein 1; KAHRP, knob-associated histidine rich protein; MESA, mature parasite-infected erythrocyte surface antigen; RESA, ring-infected erythrocyte surface antigen; PfEMP3, *Plasmodium falciparum* erythrocyte membrane protein 3; PV, parasitophorous vacuole; PEXEL, *Plasmodium* export element; VTS, vacuolar transport signal; PVM, parasitophorous vacuolar membrane; MCs, Maurer's clefts; IOV and pIOV, inside-out vesicle prepared from normal RBCs or parasite-infected RBCs; PCR, polymerase chain reaction; MBP, maltose-binding protein; PBS, phosphate-buffered saline; IB, IOV incubation buffer; BSA, bovine serum albumin; PVDF, Polyscreen® polyvinylidene difluoride; TX100, Triton X-100; DBL, Duffy binding-like domain

* Corresponding author. Tel.: +61 3 9902 9146; fax: +61 3 9902 9222.
E-mail address: brian.cooke@med.monash.edu.au (B.M. Cooke).
[1] Joint senior authors.

0005-2736/$ – see front matter © 2010 Elsevier B.V. All rights reserved.
doi:10.1016/j.bbamem.2010.01.018

respectively) and p55, and spectrin, ankyrin and band 3 link the overlying plasma membrane to the underlying membrane skeleton [7,8].

Previously, we and others have performed detailed studies to identify the interactions of numerous exported proteins that contribute to malaria's severe virulence with components of the RBC skeleton, define the specific sub-domains involved and assess their contribution to the structural and mechanical modification of IRBCs. Studies have shown that the Ring-infected Erythrocyte Surface Antigen (RESA) binds to spectrin via a 48 residue region in RESA and the repeat 16 of β-spectrin (βR16) [9,10] in an interaction that stabilises spectrin tetramers and confers both increased thermal stability on the IRBC membrane and offers a possible mechanism to suppress further merozoite invasion of the RBC [10–12]. Other studies have shown that a 19 residue region of the Mature parasite-infected Erythrocyte Surface Antigen (MESA) binds to the 30 kDa region of 4.1R in an interaction that displaces p55 from its normal interactions with 4.1R. Such interactions could thereby modulate the *in vivo* ternary 4.1R–GPC-p55 complex, altering the stability of the IRBC's membrane skeleton [13,14]. Recently, we have also shown that 14 residues of the *P. falciparum* Erythrocyte Membrane Protein 3 (PfEMP3) bind to the C-terminal EF1–2 region of α-spectrin, resulting in destabilisation of the RBC membrane skeleton [15,16]. The Knob Associated Histidine Rich Protein (KAHRP), which is required for the production of knobs on the IRBC surface [17,18], binds to spectrin, actin and ankyrin [19,20]. Recent mapping and functional studies have shown a 72 residue region of KAHRP binds to repeat 4 of α-spectrin (αR4) [21], a 91 residue region of KAHRP (which includes the 5′ repeat region) binds to ankyrin [20] and that the 3′ repeat region of KAHRP (69 residues) is required for knob production [18]. KAHRP also binds to the cytoplasmic tail (VARC region) of the major antigenic adherence protein, *P. falciparum* Erythrocyte Membrane Protein 1 (PfEMP1) [22,23], which in turn can bind spectrin and actin [19,24]. Together these KAHRP–PfEMP1–membrane skeleton interactions cluster PfEMP1 at knobs and provide the stabilizing interactions that anchor PfEMP1 in the IRBC membrane with sufficient strength to withstand the physiological shear forces exerted by circulating blood, allowing the IRBCs to adhere to the vascular endothelium *in vivo* [17].

Plasmodium falciparum Antigen 332 (Pf332) is the largest parasite protein (approx. 700 kDa) that is exported into the IRBC cytosol [25,26]. Pf332 is highly charged and possesses an extensive region of highly degenerate glutamic acid-rich repeats that span over 4300 residues (Fig. 1A; [27]). The *pf332* gene shares features common to other genes that encode exported parasite proteins, including a two exon gene structure and a *P. falciparum* protein trafficking motif (PEXEL or Vacuolar Transport Signal (VTS); [28,29]) encoded within exon 1 (Fig. 1A). Pf332 is expressed in trophozoites and is trafficked through the RBC cytosol via a Brefeldin-A sensitive secretory pathway in parasite-produced membranous structures known as Maurer's clefts (MCs). In more mature schizont parasite stages, Pf332 is found in association with the RBC membrane skeleton [25,26,30]. Recent studies have implicated Pf332 in modulating IRBC membrane rigidity, and loss of Pf332 leads to a decrease in PfEMP1 surface expression and a corresponding decrease in IRBC adhesiveness [31,32].

In this study, we have examined the association of Pf332 with the RBC membrane skeleton. Using a series of recombinant Pf332 fusion proteins in *in vitro* protein interaction assays with either inside-out vesicles (IOVs) formed from normal human RBCs or purified actin, we have broadly defined the RBC membrane skeleton binding region of Pf332 to a 260 residue region located proximal to the C-terminus of Pf332. Finer mapping studies using Triton X-100 detergent extractions of lysed and resealed RBCs incubated with Pf332 fusion proteins mapped binding domains to 86 residue and 72 residue sub-regions. Additional interaction assays demonstrated that Pf332 recombinant proteins do not bind to spectrin. Rather, actin co-sedimentation assays demonstrated that the 260 residue region of Pf332 bound in a specific and saturable manner to F-actin ($K_d = 0.60$ μM) at a binding site not shared with another known actin-binding malaria protein. The continued elucidation of protein interactions at the IRBC membrane skeleton will facilitate construction of a detailed protein interaction model and increase our understanding of the complex structural and mechanical modifications of IRBCs that ultimately result in the severe clinical manifestations of *P. falciparum* malaria.

2. Materials and methods

2.1. Parasite culture

Plasmodium falciparum parasites (3D7 line) were cultured *in vitro* and synchronized using sorbitol as previously described [33].

2.2. Construction of pMAL-c2 clones, and expression and purification of recombinant proteins

Specific oligonucleotide primers (Table 1) were designed with reference to the *pf332* nucleotide sequence [30,34] and used to PCR amplify regions of *pf332* from *P. falciparum* 3D7 genomic DNA. PCR products were cloned into the pMAL-c2 Maltose-Binding Protein (MBP) expression plasmid (New England Biolabs, USA) using GATEWAY™ Cloning Technology (Invitrogen, USA) and the nucleotide sequence of each clone was confirmed by automated DNA sequencing. MBP–Pf332 fusion proteins were expressed, purified, dialysed against phosphate-buffered saline (PBS; 10 mM Na_2HPO_4/NaH_2PO_4, pH 7.4, containing 0.15 M NaCl) and concentrated by centrifugal filtration as previously described [15]. Total protein concentrations were determined by Bio-Rad Protein Assays (Bio-Lab Laboratories, USA). The isoelectric points (pI) of each MBP–Pf332 fusion protein and rabbit actin were determined using http://ca.expasy.org/tools/pi_tool.html.

2.3. In vitro binding assays using IOVs

Inside-out vesicles (IOVs) were prepared for use in binding assays from normal human RBCs using previously described methods [15]. For the binding assays, prepared IOVs diluted in IOV Incubation Buffer (IB; 138 mM NaCl, 5 mM KCl, 6 mM Na_2HPO_4, 5 mM glucose, pH9.0) were used to coat wells of 96 well microtiter plates (Dynatech Laboratories Inc., USA) overnight at 4 °C. Wells were then blocked overnight at 4 °C with 5% (w/v) Bovine Serum Albumin (BSA) in IB, before washing twice with IB. Then, 0.5–4 μg of total recombinant MBP–Pf332 fusion protein diluted in IB containing 0.05% (v/v) Tween 20 was added to each well and incubated overnight at 4 °C. Wells were washed 5 times with IB before proteins were stripped from the wells using heated (70 °C) reducing sample buffer. Proteins were resolved by SDS-PAGE in 10% (w/v) polyacrylamide gels and transferred to Polyscreen® polyvinylidene difluoride (PVDF) membrane (NEN® Life Science Products Inc., USA). Interacting proteins were detected by immunoblotting using a primary polyclonal rabbit anti-MBP antiserum [15] and secondary anti-rabbit Ig-horseradish peroxidase conjugate (Silenus Labs Pty. Ltd., Australia). Autoradiographic images were obtained using NEN Renaissance™ Western Blot chemiluminescence reagent (NEN® Life Science Products Inc., USA).

IOVs were also prepared from 3D7 *P. falciparum*-IRBCs (pIOVs). Briefly, mature stage IRBCs were purified from culture by Percoll Density Gradient Centrifugation [35]. Isolated IRBCs were then treated identically to that described above for the preparation of IOVs from normal human RBCs [15]. pIOVS were then resuspended in IOV Incubation Buffer and used in immunoblots.

The specificity and saturability of the interaction between Pf332-F19 and IOVs was demonstrated by incubating serial dilutions of MBP–Pf332-F19 protein (titrated from 5 μM to 0.0 μM) with IOVs in

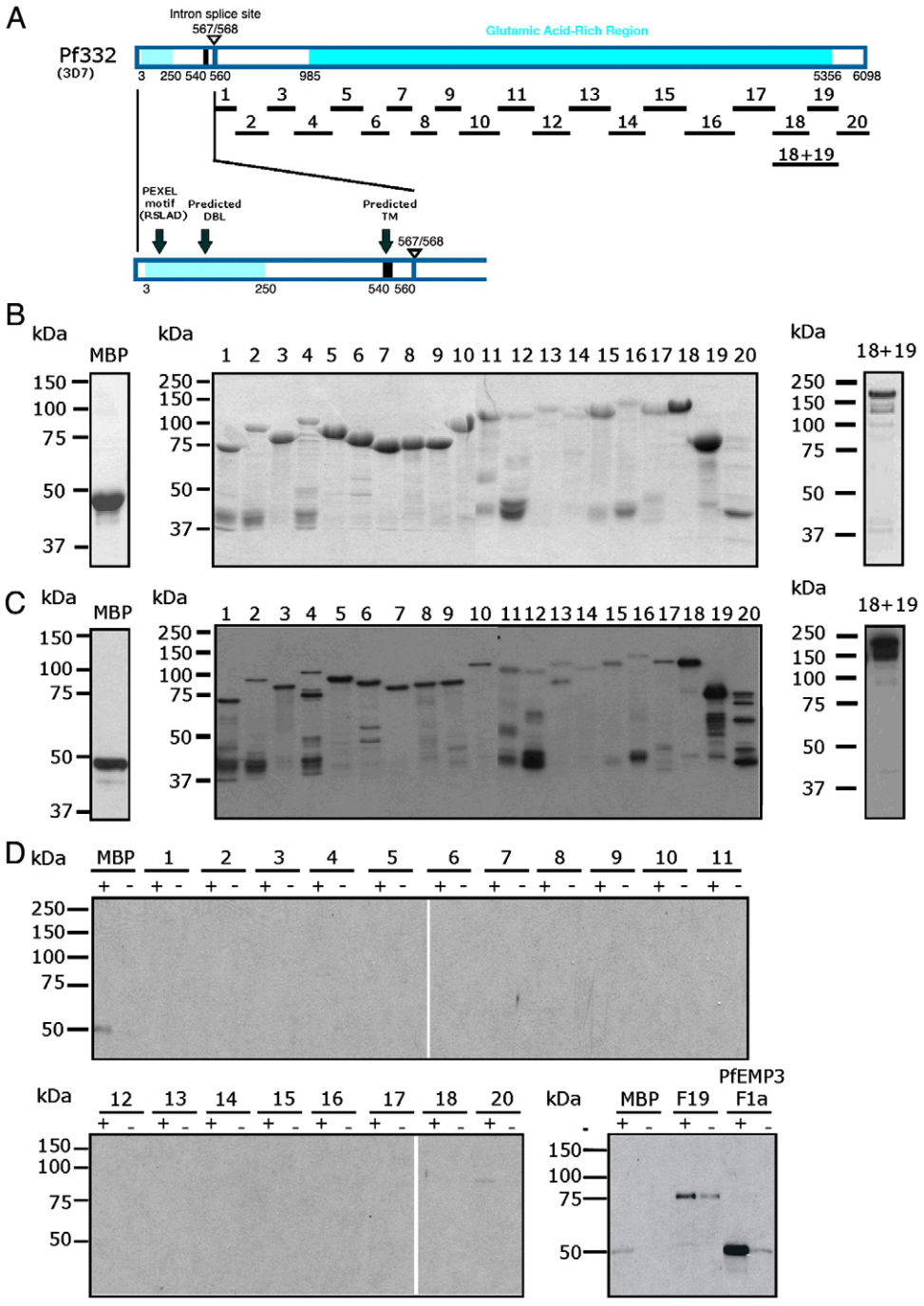

Fig. 1. Mapping the region of Pf332 that binds the RBC membrane skeleton. A. Schematic representation of full length Pf332 protein. The *pf332* gene is comprised of two exons separated by an intron [30]. Residues 1–567 are encoded by the first exon of the *pf332* gene and encodes a PEXEL motif (RSLAD), a Duffy Binding-Like domain (DBL; light shaded region) and a predicted transmembrane spanning domain (TM). Residues 568–6098 are encoded by the second exon of the *pf332* gene and encode an extensive glutamic acid-rich region (darker shaded region). The relative locations of the twenty one fragments (F1 through F20, plus F18+19) that were expressed and purified as MBP fusion proteins and together represent the Pf332 protein sequence encoded by the second exon of *pf332* are shown below the protein schematic. Relevant amino acid residue numbers are shown adjacent to the schematic. B. Purified MBP–Pf332 fusion proteins. 2 μg (total protein) of each purified protein was resolved by SDS-PAGE and stained with Coomassie Brilliant Blue. The proteins are indicated by the protein fragment number above each lane. C. Each of the purified MBP–Pf332 fusion proteins (50 ng total protein) was immunoblotted with anti-MBP antiserum to confirm the presence of the N-terminal MBP tag and demonstrate the apparent molecular mass of each protein when immunoblotted. D. IOV binding assay immunoblots. Samples stripped from IOV-coated wells (lanes headed by '+') and BSA-coated wells (lanes headed by '−') are indicated. The name of each Pf332 protein fragment analysed is shown above each pair of lanes. Pf332-F19 bound to IOVs, with only residual levels observed binding to BSA. The interaction positive control protein MBP–PfEMP3-F1a bound to IOVs and at much lower levels to BSA. MBP showed only residual binding to IOVs and did not bind to BSA. The immunoblotted assay samples, although separated into multiple panels here, were derived under identical and simultaneous experimental conditions.

an IOV binding assay. Proteins stripped from the wells were resolved by SDS-PAGE and transferred to PVDF and immunoblotted with anti-MBP antiserum. The resulting autoradiographic data was analysed by densitometry using the public domain NIH Image program (http://rsb.info.nih.gov/nih-image/). A saturation of binding curve was constructed from the densitometric data of a representative binding assay after subtraction of the signal obtained for the presence of residual MBP–Pf332–F19 binding to BSA. The concentration at which

Table 1
Oligonucleotide primers sequences.

Fragment	Isoelectric point (pI)[a]	Primer[b]	Sequence (5′→3′)[c]
F1	4.29	p1 (+)	ggggacaagtttgtacaaaaaagcaggcttagaattcCATTCTTTGATTGATCGTGTTC
		p2 (−)	ggggaccactttgtacaagaaagctgggtcgaattcAATTAATTGACCTTTAAATGTA
F2	4.00	p3 (+)	ggggacactttgtacaagaaagctgggtcgaattcTTTAAAGGTCAATTAATTAACGA
		p4 (−)	ggggaccacagtttgtacaaaaaagcaggcttagaattcATTTTCTTTGTCTCGAACGTCA
F3	3.97	p5 (+)	ggggacaagtttgtacaaaaaagcaggcttagaattcAACGATGACGTTCGAGACAAA
		p6 (−)	ggggaccactttgtacaagaaagctgggtcgaattcTGCTCCTTCTTCTTCTACAACTTCC
F4	3.96	p7 (+)	ggggacaagtttgtacaaaaaagcaggcttagaattcATAGTAGAAGATGAAGCATCAGTC
		p8 (−)	ggggaccactttgtacaagaaagctgggtcgaattcTTCATTGTCTTCATTAATCAAACC
F5	4.05	p9 (+)	ggggacaagtttgtacaaaaaagcaggcttagaattcAAAGAAGAATTAATTACTGAAATG
		p10 (−)	ggggaccactttgtacaagaaagctgggtcgaattcTGGAGTATGTTCATTAATAATATC
F6	4.00	p11 (+)	ggggacaagtttgtacaaaaaagcaggcttagaattcCCATTAGAAGAAACGAAAATTG
		p12 (−)	ggggaccactttgtacaagaaagctgggtcgaattcGCTAACTGATCCAATATCTTT
F7	4.09	p13 (+)	ggggacaagtttgtacaaaaaagcaggcttagaattcGTTAAAGATATTGGATGAGTTAG
		p14 (−)	ggggaccactttgtacaagaaagctgggtcgaattcTCCTTCATACTGTACAGC
F8	3.97	p15 (+)	ggggacaagtttgtacaaaaaagcaggcttagaattcACAGAAGAAGCTGTACAGTATG
		p16 (−)	ggggaccactttgtacaagaaagctgggtcgaattcCGTAATCGATCCTTCTCCA
F9	4.16	p17 (+)	ggggacaagtttgtacaaaaaagcaggcttagaattcGGAGAAGGATCGATTACG
		p18 (−)	ggggaccactttgtacaagaaagctgggtcgaattcTACGACTTCTTCAGTTACTGTTG
F10	3.69	p19 (+)	ggggacaagtttgtacaaaaaagcaggcttagaattcGAAATAGTGGACGAAGTGTCTC
		p20 (−)	ggggaccactttgtacaagaaagctgggtcgaattcTTCCCCATTAACGGATTCAGA
F11	3.91	p21 (+)	ggggacaagtttgtacaaaaaagcaggcttagaattcTCTGAATCCGTTAATGGG
		p22 (−)	ggggaccactttgtacaagaaagctgggtcgaattcTATTTTTTCAGTAAGTGATTTTTCG
F12	3.87	p23 (+)	ggggacaagtttgtacaaaaaagcaggcttagaattcAAAGAAATAATTGACGAAAAATCAC
		p24 (−)	ggggaccactttgtacaagaaagctgggtcgaattcTTTCTCAATCCATACATTTTC
F13	3.84	p25 (+)	ggggacaagtttgtacaaaaaagcaggcttagaattcAATGTATGGATTGAGAAAGAA
		p26 (−)	ggggaccactttgtacaagaaagctgggtcgaattcTGATCCTTGTTGTACAACTTT
F14	3.80	p27 (+)	ggggacaagtttgtacaaaaaagcaggcttagaattcCAGGAAGAATCTCATGTTGAAA
		p28 (−)	ggggaccactttgtacaagaaagctgggtcgaattcAATATCTTCAGTAATTGATTCG
F15	3.90	p29 (+)	ggggacaagtttgtacaaaaaagcaggcttagaattcAAAATCGAATCAATTACTGAAGAT
		p30 (−)	ggggaccactttgtacaagaaagctgggtcgaattcAGTAAAAGATCCACCTTGTAT
F16	3.83	p31 (+)	ggggacaagtttgtacaaaaaagcaggcttagaattcGAAATAATACAAGGTGGATATT
		p32 (−)	ggggaccactttgtacaagaaagctgggtcgaattcATTAAAAGACCCTTCTTCTAA
F17	3.84	p33 (+)	ggggacaagtttgtacaaaaaagcaggcttagaattcGTAGAAGAAGGATCAGATACG
		p34 (−)	ggggaccactttgtacaagaaagctgggtcgaattcCATAATTTTATAATTAAGGGC
F18	4.38	p35 (+)	ggggacaagtttgtacaaaaaagcaggcttagaattcGATAAAGCCCTTAATGAG
		p36 (−)	ggggaccactttgtacaagaaagctgggtcgaattcGTCATTGGCAGATTTATTTG
F19	4.77	p37 (+)	ggggacaagtttgtacaaaaaagcaggcttagaattcAATGATACTGTAATGGTTAT
		p38 (−)	ggggaccactttgtacaagaaagctgggtcgaattcAAGTTCATCGTACTTAAATTG
F20	5.49	p39 (+)	ggggacaagtttgtacaaaaaagcaggcttagaattcAAATATGCTAAGAAAAGATTT
		p40 (−)	ggggaccactttgtacaagaaagctgggtcgaattcGTTCTCATTTACACTAAATTC
F19a	5.67	p41 (+)	ccgggaaggatttcaAATGATACTGTAATGGTTATAAAAATC
		p42 (−)	cgggaattcATTCCTCATATCGATTTTCAAATC
F19b	4.83	p43 (+)	ccgggaaggatttcaACATATGAAAGCGATCAAAATGAC
		p44 (−)	cgggaattcTTCCTGTAATACATTACTGACATC
F19c	4.86	p45 (+)	ccgggaaggatttcaAATGCATCAGAAGCTTCTGTTG
		p38 (−)	ggggaccactttgtacaagaaagctgggtcgaattcAAGTTCATCGTACTTAAATTG
F18+19	4.66	p35 (+)	ggggacaagtttgtacaaaaaagcaggcttagaattcGATAAAGCCCTTAATGAG
		p38 (−)	ggggaccactttgtacaagaaagctgggtcgaattcAAGTTCATCGTACTTAAATTG

Oligonucleotide primers sequences used in the construction of the *pf332* DNA fragments.
[a] The isoelectric points (pI) of each MBP–Pf332 fusion protein and rabbit actin were determined using http://ca.expasy.org/tools/pi_tool.html. The pI of rabbit actin is 5.24.
[b] (+) and (−) refer to coding (forward) and non-coding (reverse) DNA sequences, respectively.
[c] Gene specific sequence shown in uppercase; non-complimentary sequence shown in lower case and enzyme restriction sites are underlined.

binding was half saturated (K_d) was determined by regression analysis of the saturation of binding curve data.

2.4. In vitro binding assays using spectrin

Spectrin-binding assays were performed in a similar manner to the IOV binding assays, with some modifications. Briefly, PBS was used instead of IB and 100 ng of purified human spectrin (Sigma, Australia) was used to coat the wells of a 96 well microtitre plate (Dynatech Laboratories Inc., USA). Assays were then processed as described above.

2.5. Triton X-100 detergent solubility

Triton X-100 (TX100) detergent extractions were performed on *P. falciparum* 3D7 parasites harvested to more than 99% trophozoite stage IRBCs by Percoll Density Gradient Centrifugation [35]. Then, 45 μl of purified IRBCs was extracted in 1.5 ml PBS containing 1% (v/v) TX100 in the presence of protease inhibitor solution (Roche Diagnostics, Australia) for 10 min on ice. Samples were centrifuged at 12,000×*g* for 5 min at 4 °C before removal of the supernatant. The TX100 insoluble pellet was then washed in PBS/TX100/protease inhibitor solution before resuspension of the pellet and supernatant fractions in reducing protein sample buffer. A sample of the resultant TX100 insoluble 3D7 parasite fraction was resolved in 0.5% (w/v) agarose/3.0% (w/v) acrylamide gels [36] alongside samples of IOVs (prepared from normal human RBCs), pIOVs (prepared from 3D7 *P. falciparum*-IRBCs) and Cross-linked SDS Molecular Weight Markers (Sigma, Australia) using a Mini-PROTEAN® III Cell apparatus (Bio-Rad). Samples were then transferred to PVDF membrane and immunoblotted with rabbit polyclonal anti-Pf332 antiserum (1:300 dilution; K. Berzins, Stockholm University, Sweden).

TX100 detergent solubilities were also performed on lysed and resealed RBCs pre-incubated with MBP–Pf332 fusion proteins, MBP

alone or with MBP–PfEMP3-F1a or -F5 (positive and negative binding control proteins, respectively [15]). Lysis and resealing was performed as previously described [15]. The resultant samples were then resolved in 12% (w/v) polyacrylamide gels, before immunoblot detection using polyclonal rabbit anti-MBP antiserum.

2.6. Actin co-sedimentation assays

Actin co-sedimentation assays were used to demonstrate the specificity and saturability of the interaction between Pf332 and F-actin, and were performed as previously described [15]. Briefly, monomeric G-actin (Cytoskeleton, Denver CO, USA; ≥95% pure by SDS-PAGE analysis) was polymerised to F-actin. F-actin (5 μM) was then interacted with Pf332-F19 (titrated from 5 μM to 0.0 μM) alongside the negative interaction control proteins MBP–Pf332-F7 and MBP alone (both 5.0 μM) [15]. Pellet and supernatant fractions were resolved proteins by SDS-PAGE in 10% (w/v) polyacrylamide gels before transfer to PVDF for immunoblot detection using polyclonal anti-MBP antiserum. Equal loading of pellet and supernatant samples was demonstrated by probing duplicate blots with monoclonal anti-actin antibodies (Sigma, Australia). The resulting autoradiographic data was analysed by densitometry (see above). A saturation of binding curve was constructed from the densitometric data obtained from a representative co-sedimentation experiment after subtraction of the signal obtained for the presence of non-binding MBP–Pf332-F7 in the pellet. The half saturation concentration (K_d) was determined by regression analysis of the saturation of binding curve data.

Inhibition of binding to actin co-sedimentation assays were performed to determine if the binding of either MBP–PfEMP3-F1a or MBP–Pf332-F19 to F-actin inhibited the binding of the other to actin. These assays were performed as described above for actin co-sedimentation assays except that F-actin (5 μM) was added to either MBP–PfEMP3-F1a (5 μM) or MBP–Pf332-F19 (5 μM) prior to addition of the other protein (titrated from 5.0 to 0.0 μM) and subsequent incubation for an hour at room temperature. Protein mixtures were then ultracentrifuged and the resultant pellet and supernatant fractions collected, resolved by SDS-PAGE in 10% (w/v) polyacrylamide gels and immunoblotted using either polyclonal anti-MBP antiserum or monoclonal anti-actin antibodies, as described above. Additional inhibition co-sedimentation assays were performed in which F-actin (5 μM) was pre-incubated for 1 h with either MBP–PfEMP3-F1a (5 μM) or MBP–Pf332-F19 (5 μM), prior to the addition the other protein (titrated from 5.0 to 0.0 μM) and subsequent incubation for a further hour at room temperature. Assays were then processed and analysed as described above.

3. Results

3.1. Cloning, protein expression and purification

The *P. falciparum pf332* gene has a two exon gene structure and encodes a PEXEL/VTS motif (RSLAD; residues 77–81) in its first exon [30]. Sequences encoded by the first exon were excluded from our analyses because current membrane topology predictions place the N-terminal 540 residues of Pf332, which are located upstream of the predicted transmembrane domain (Fig. 1A), within the MCs during trafficking of Pf332 to the RBC membrane before subsequent exposure on the IRBC membrane surface [30]. In either of those locations, the 540 residues would be unavailable for binding to the RBC membrane skeleton. Given the unusually large size of the *pf332* second exon, which encodes some 5530 residues and is largely comprised of a highly repetitive glutamic acid-rich region (approx. 4300 residues; Fig. 1A), it was not feasible to clone and express recombinant Pf332 proteins from a full length *pf332* second exon DNA fragment. Instead, defined fragments that together represent the entire second exon of the *pf332* gene were PCR amplified, cloned into the pMALc2 vector, sequenced and used to express and purify MBP–Pf332 fusion proteins. The purified MBP–Pf332 fusion proteins that were used in initial interaction assays are shown in Fig. 1B. Immunoblot detection using polyclonal anti-MBP antisera was performed on all purified MBP–Pf332 fusion proteins to demonstrate the presence of the MBP tag and confirm the identity of each protein (Figs. 1C and 3C).

3.2. Mapping the Pf332 RBC membrane skeleton binding domain

Inside-out vesicles (IOVs) were prepared from normal human RBCs and used in binding assays. A sample of prepared IOVs resolved by SDS-PAGE and stained with Coomassie Brilliant Blue confirmed the presence of the major RBC membrane skeleton proteins, including spectrin and actin (data not shown).

An initial series of IOV binding assays using the MBP–Pf332 fusion proteins -F1 through -F20 mapped the general region of Pf332 that binds to the RBC membrane skeleton. Representative immunoblots are shown in Fig. 1C. Pf332-F19 bound to IOVs, but only residual levels were detected binding to BSA. The positive control MBP–PfEMP3-F1a.1, a known IOV binding protein fragment [15], also bound to IOVs, and only minimally to BSA. MBP alone failed to bind to BSA, and only extremely low levels were detected interacting with IOVs. These initial interaction assays identified a 260 residue region of Pf332 encoded by the second exon of the *pf332* gene as the region of Pf332 that binds to the RBC membrane skeleton.

A parallel set of assays interacted Pf332 fusion proteins with membrane skeleton proteins maintained in the intact RBC and took advantage of the fact that proteins linked to the RBC membrane skeleton, including Pf332, are typically insoluble in non-ionic detergents such as Triton X-100 (TX100; [37]) (Fig. 2B). In these assays, resealed RBCs that had been pre-incubated with purified MBP–Pf332 fusion proteins, MBP alone or with the interaction control proteins MBP–PfEMP3-F1a or -F5 (positive and negative binding proteins respectively; [15]) were extracted with TX100 and the resultant TX100 soluble and insoluble fractions immunoblotted with anti-MBP antiserum (Fig. 2C). Data from these assays confirmed that the 260 residue -F19 region of Pf332 bound to the RBC membrane skeleton. This experiment also indicated the presence of binding residues contained within -F18, the region that is located immediately upstream of -F19. We also generated a -F18+19 fusion protein (Fig. 1B and C), in which the -F18 and 19 regions were contained in the same contiguous fusion protein, and confirmed its ability to bind to the RBC membrane skeleton (Fig. 2C).

3.3. Finer mapping of the membrane skeleton binding region of Pf332

To further define the residues within Pf332-F19 that bind to the RBC membrane skeleton, we generated smaller non-overlapping sub-fragment MBP fusion proteins (Fig. 3A, B and C). Representative immunoblots of TX100 extracted resealed RBCs pre-incubated with either -F19, -F19a, -F19b or -F19c (Fig. 3D) mapped the binding residues of -F19 to the N-terminal 86 residues that are present in -F19a. Downstream sequences that are located within the 72 residue -F19c region were also observed to possess some binding to the RBC membrane skeleton however, no binding was detected with -F19b but this may reflect the relatively poor quality of the full length protein generated rather than the lack of binding sequences in -F19b. To demonstrate the specificity and saturability of this -F19–IOV interaction, serial dilutions of MBP–Pf332-F19 were interacted with IOVs, and the resultant immunoblot data from a representative assay was analysed by densitometry and graphed as a saturation of binding curve (Fig. 3D). Using regression analysis of the saturation curve data, the half saturation concentration (K_d) was determined to be $K_d = 0.40$ μM.

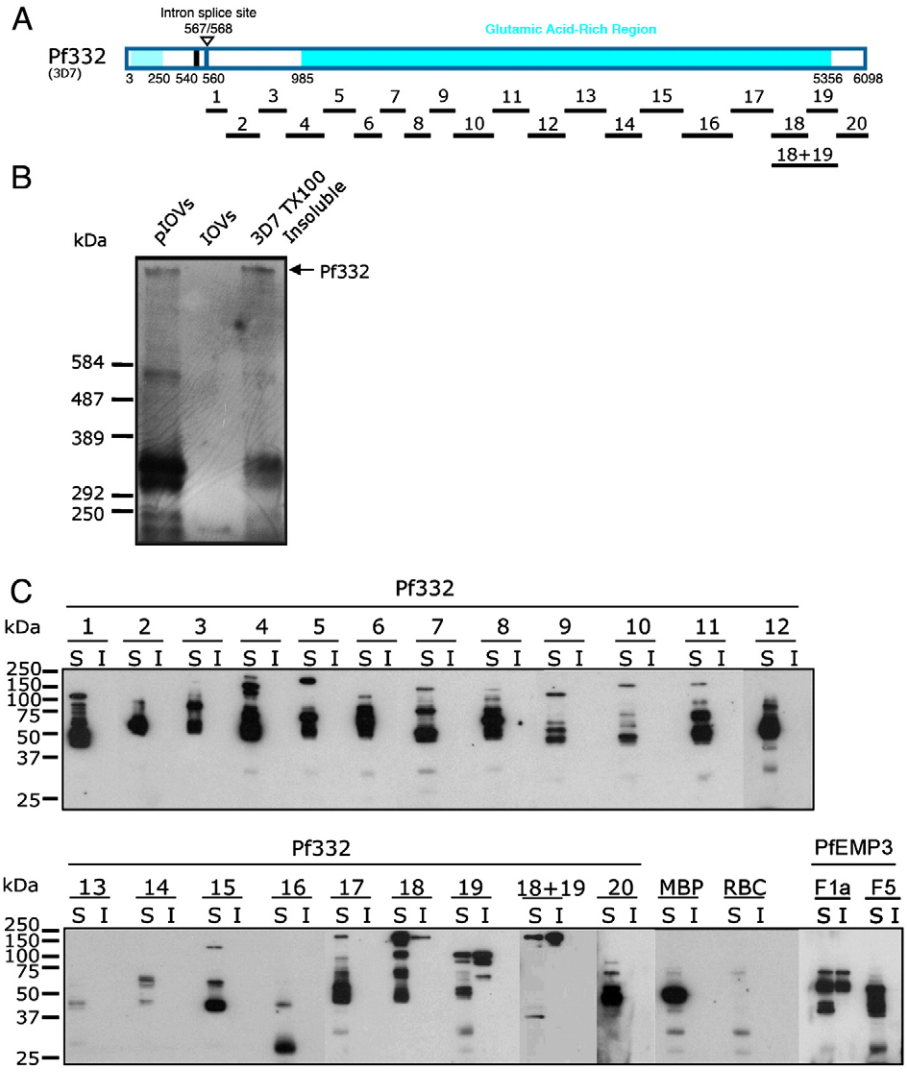

Fig. 2. RBC membrane skeleton association of Pf332. A. Schematic representation of full length Pf332 protein showing the relative locations of the twenty one Pf332 fragments investigated. B. Immunoblot detection of Pf332 in *P. falciparum*-IRBCs extracted with Triton X-100. Samples of IOVs and IOVs prepared from *P. falciparum*-IRBCs (pIOVs) were resolved alongside the TX100 insoluble fraction of *P. falciparum* 3D7 parasites in 0.5% (w/v) agarose/3.0% (w/v) acrylamide gels [36], before transferring to PVDF membrane and immunoblotting with anti-Pf332 antiserum. Pf332 was detected as a band of >584 kDa (indicated by the arrow) in the 3D7 TX100 insoluble fraction and in the pIOVs sample, but not in the IOVs prepared from normal human RBCs. Although originally described as a megadalton protein [25,27], Pf332 is currently predicted to be a 700 kDa protein, and was observed in our hands as having a molecular mass in excess of 584 kDa. It is not uncommon for highly charged repetitive malaria proteins, such as Pf332, to resolve at anomalous higher-than-predicted molecular masses in SDS-PAGE [47]. C. TX100 extractions were preformed on lysed and resealed RBCs that had been incubated with 5 μM purified MBP–Pf332 fusion proteins, MBP alone, or with the binding control proteins MBP–PfEMP3 fusion proteins F1a or F5 (RBC membrane skeleton binding and non-binding regions, respectively; [15]). The TX100 soluble (S) and insoluble (I) fractions were resolved by SDS-PAGE and immunoblotted with anti-MBP antiserum. MBP–Pf332-F19 was detected in both the soluble and insoluble fractions. The region adjacent to -F19, -F18, was also detected in the insoluble fraction, but at lower levels than -F19. When -F18 and -F19 were combined into the same contiguous fusion protein (-F18+19), the protein was also detected in the insoluble fraction. As expected, the RBC membrane binding control protein MBP–PfEMP3-F1a was present in both the soluble and insoluble fractions, whereas the non-binding MBP–PfEMP3-F5 protein and MBP alone were present only in the soluble fractions. No significant immunoreactivity was observed in either fraction for TX100 extracted RBCs lysed and resealed in the absence of MBP or other MBP fusion proteins. The diversity of protein sizes and the number of bands per protein sample are reflective of the sizes of the Pf332 gene fragments expressed as MBP fusions, differences in their coding sequences, and the ability of *E. coli* to express these gene fragments as full length proteins.

3.4. Pf332 binds to actin

To determine if the -F19 region of Pf332 binds to the RBC membrane skeleton via interactions with actin, co-sedimentation assays were performed using polymerised F-actin. Under the sedimentation conditions used, monomeric actin (G-actin) would be typically found in the supernatant, whereas F-actin would be located in the pellet [15]. In these assays, -F19 bound to F-actin and was detected in the pelleted fractions (Fig. 4A). The specificity and saturability of the interaction between F-actin and -F19 proteins was demonstrated by incubating constant F-actin (5.0 μM) with titrated serial dilutions of -F19 (from 0.0 μM to 5.0 μM) or the negative control proteins MBP–Pf332-F7 or MBP alone (5.0 μM). Immunoblots of representative experiments are shown (Fig. 4A). Due to the polymeric nature of F-actin, sensitive resonance mirror detection measurements to determine the kinetics of the actin–MBP–Pf332-F19 interaction were not possible. However, the kinetics of the actin–MBP–Pf332-F19 interaction could be estimated from the saturation of binding curve for -F19 binding to F-actin (Fig. 4C). The corresponding densitometric data was corrected by subtraction of the relative amount of MBP–Pf332-F7 pelleted in the absence of F-actin and graphed. Using regression analysis of the saturation curve data, the half saturation concentration (K_d) was determined to be $K_d = 0.60$ μM.

3.5. Pf332 does not bind to spectrin

To determine whether Pf332 bound to spectrin, we performed binding assays between the MBP–Pf332-F19 and purified spectrin

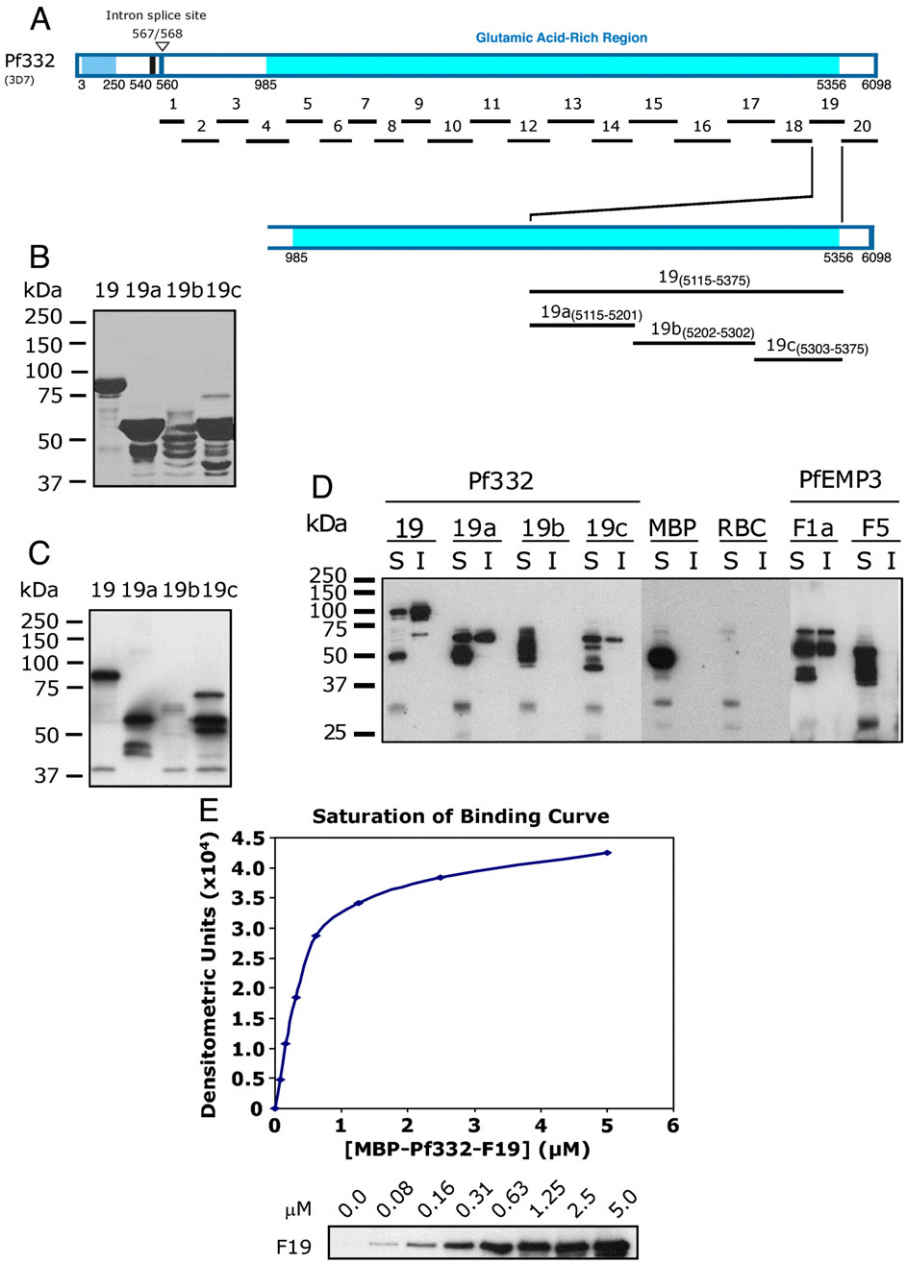

Fig. 3. Finer mapping of residues in Pf332-F19 that bind to the RBC membrane skeleton. A. Schematic representation of full length Pf332 protein showing the relative locations on the twenty fragments investigated. To further define the binding residues contained within the 260 residue -F19 region, three smaller non-overlapping sub-fragments (-F19a, -F19b and -F19c) were expressed and purified as MBP fusion proteins. B. Purified MBP–Pf332 F19 sub-fragment fusion proteins. 2 μg (total protein) of each purified protein was resolved by SDS-PAGE before staining with Coomassie Brilliant Blue. C. Each of the MBP–Pf332 F19 sub-fragment fusion proteins (50 ng total protein) was immunoblotted with anti-MBP antiserum to confirm the presence of the N-terminal MBP tag and demonstrate the apparent molecular mass of each protein when immunoblotted. D. The TX100 soluble (S) and insoluble (I) fractions of lysed and resealed RBCs that had been incubated with 5 μM fusion protein were resolved by SDS-PAGE and immunoblotted with anti-MBP antiserum. MBP–Pf332-F19, and its sub-fragment proteins -F19a and -F19c were both detected in the Tx100 soluble and insoluble fractions, whereas the intervening sub-fragment -F19b was not. Neither MBP nor MBP–PfEMP3-F5 was detected in the insoluble fractions, whereas MBP–PfEMP3-F1a was. Together, these data map a membrane skeleton binding region of Pf332 to the 86 residues of -F19a. These data also suggest the presence of other residues within the downstream 72 residues of -F19c that may contribute to the overall protein interaction of Pf332 with the membrane skeleton. E. A saturation of binding curve was constructed from the densitometric data obtained from a representative IOV binding assay using serial dilutions of MBP–Pf332-F19 protein (titrated from 5.0 to 0.0 μM; panel below the graph). The half saturation concentration (K_d) was determined to be $K_d = 0.40$ μM.

(data not shown). In these assays, only background amounts of -F19 bound to spectrin at levels comparable to the negative interaction control BSA. A spectrin-binding positive control interaction was simultaneously performed using MBP fused to the spectrin-binding region of PfEMP3 (MBP–PfEMP3-F1a.1; [15]). MBP–PfEMP3-F1a.1 bound to spectrin but not to BSA. Taken together with the actin pelleting experiments above, it appears that Pf332 binds to the RBC membrane skeleton via specific interactions with actin but not spectrin (data not shown).

3.6. PfEMP3-F1a and Pf332-F19 bind to different regions of F-actin

To determine if either of the actin-binding regions that we have identified in PfEMP3 [15] or Pf332 were able to bind the same residues in actin, we performed inhibition of binding to actin co-sedimentation assays. In these assays, we added F-actin (5 μM) to either MBP–PfEMP3-F1a (5 μM) or MBP–Pf332-F19 (5 μM), and then added the other protein (titrated from 20 μM to 0.0 μM). A representative experiment is shown in Fig. 5. Neither increasing concentrations of

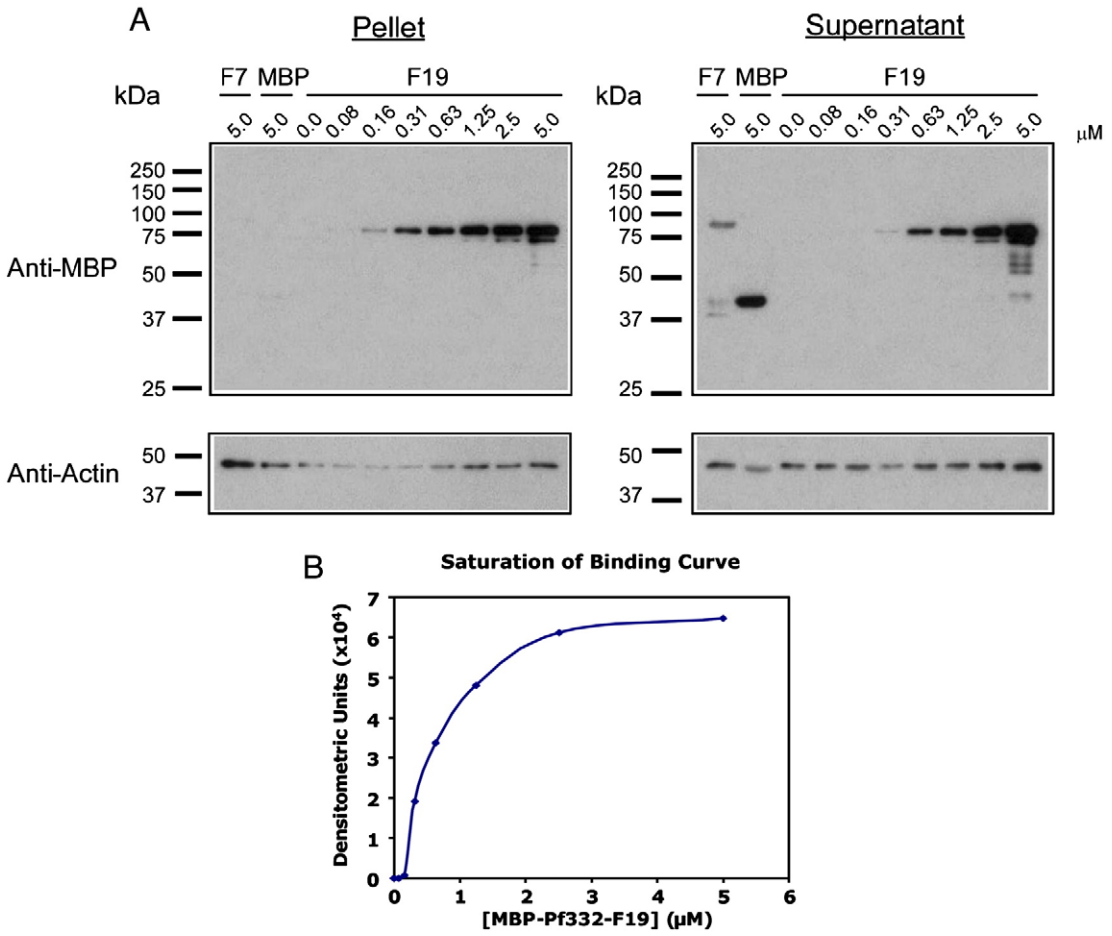

Fig. 4. Pf332-F19 binding to actin is saturable and specific. A. Actin co-sedimentation assays were performed using polymerised F-actin. Constant concentrations of F-actin (5 μM) were incubated with titrated serial dilutions of MBP–Pf332-F19 and centrifuged. The pellet and supernatant fractions were analysed by immunoblotting with anti-MBP and anti-actin antibodies and subsequent densitometry. MBP–Pf332-F19 pelleted with F-actin, whereas the non-binding MBP and MBP–Pf332-F7 proteins remained in the supernatant. B. A saturation of binding curve was constructed from the densitometric data obtained from a representative actin co-sedimentation assay using MBP–Pf332-F19 protein (panel A). The half saturation concentration (K_d) was determined to be $K_d = 0.60$ μM.

MBP–PfEMP3-F1a nor MBP–Pf332-F19 was able to inhibit the binding of the other protein to F-actin under these assay conditions. In both instances, only residual levels of the negative interaction control proteins MBP (5.0 μM), MBP–Pf332-F7 (5.0 μM) and MBP–Pf332-F5 (5.0 μM) pelleted with F-actin. The positive interaction controls MBP–PfEMP3-F1a (5.0 μM) and MBP–Pf332-F19 (5.0 μM) each pelleted with F-actin as expected (Fig. 5). Additionally, we also conducted inhibition of co-sedimentation assays in which F-actin (5 μM) was pre-incubated with either MBP–PfEMP3-F1a (5 μM) or MBP–Pf332-F19 (5 μM) for 1 h prior to the addition of the other protein (titrated from 20 μM to 0.0 μM) and further incubation (data not shown). No discernable difference was observed in experimental outcome resulting from assays in which F-actin had or had not been pre-incubated with a binding partner prior to the addition of serially titrated third protein (data not shown). Taken together, these data demonstrate that PfEMP3-F1a and Pf332-F19 are not able to displace each other from binding to actin, and thus bind to physically distinct regions within actin.

4. Discussion

Pf332 is synthesized by the intracellular malaria parasite and exported to the RBC via MCs where it associates with the RBC membrane skeleton [25,26]. The current membrane topology of Pf332 predicts that the N-terminal 540 residue region of Pf332 (encoded by exon 1; Fig. 1A) is located in either in the lumen of an organelle (the MC) or extracellularly exposed on the IRBC [30]. This prediction seems reasonable as this domain contains a Duffy Binding-Like (DBL) domain which is rich in cysteine residues that are likely to form numerous disulphide bonds, which can only occur in an oxidizing environment found inside trafficking organelles or extracellularly. Therefore, the sequences encoded by exon one of *pf332* would not be present within the same biological compartment as the RBC membrane skeleton. Hence, our protein interaction studies focused specifically upon the residues downstream of the transmembrane spanning domain (Fig. 1A) that are encoded by the second exon of the *pf332* gene and are predicted to reside entirely within the RBC cytosol [30].

Here, using two independent *in vitro* interaction methods that utilize properly conformed RBC membrane skeletons, we have mapped the membrane skeleton binding domain of Pf332 to a 260 residue region located proximal to its C-terminus. Actin co-sedimentation assays further demonstrated that this 260 residue region of Pf332 binds to actin in a specific and saturable manner with moderate affinity. Additional mapping studies refined the binding region predominantly to an 86 residue region encompassed by the -F19a sub-region of Pf332 (residues 5155–5201), although other residues (located in -F18 and -F19c) seem to provide some weaker contribution to the overall interaction. The presence of binding sequences encoded in -F19b however, cannot be ruled out because despite numerous attempts of optimise the yield of -F19b full length fusion protein, the relative quality of the -F19b used was poor when

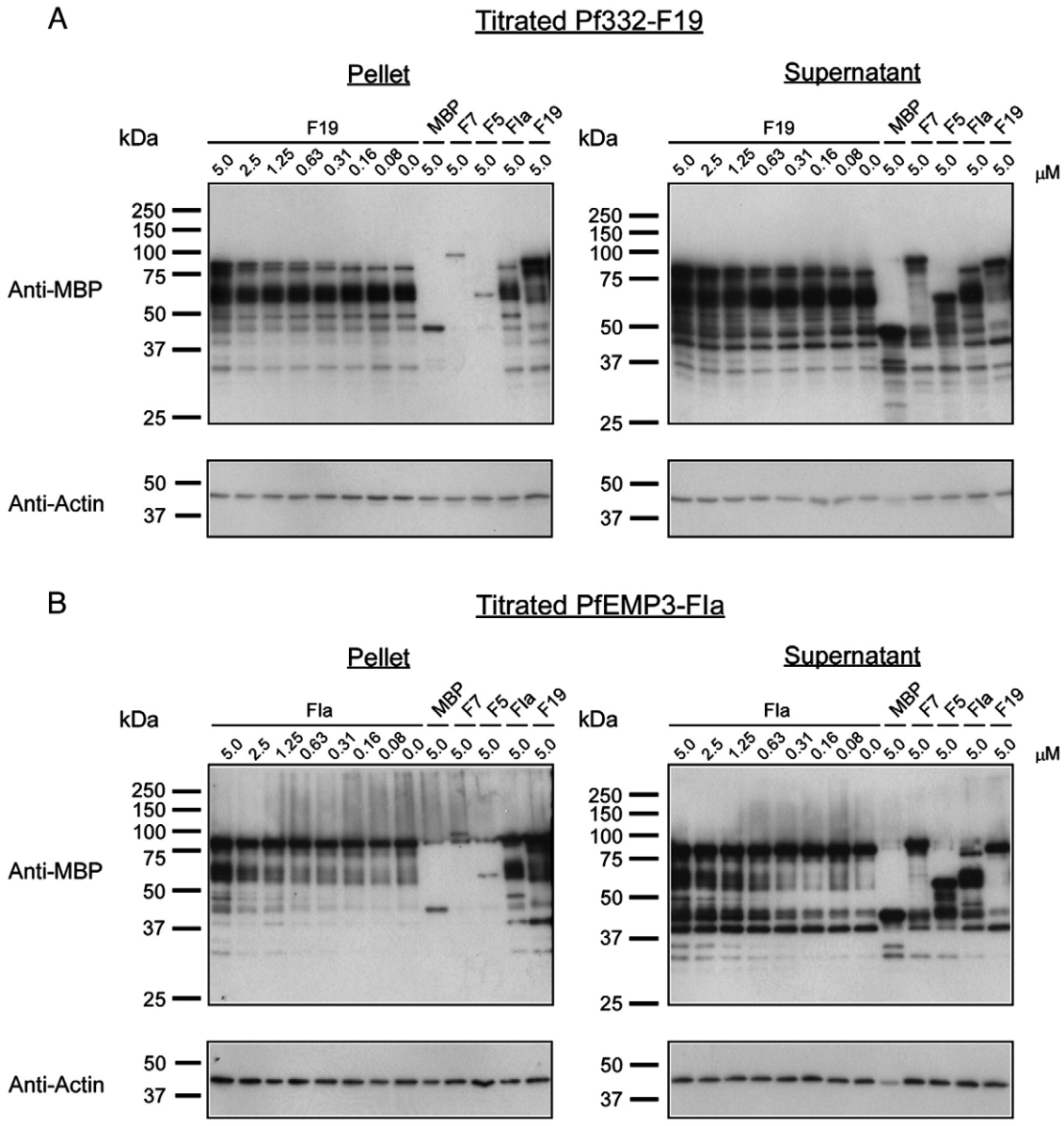

Fig. 5. PfEMP3-F1a and Pf332-F19 bind to different regions of F-actin. Inhibition of binding to actin co-sedimentation assays were performed to determine if MBP–PfEMP3-F1a or MBP–Pf332-F19 bound to the same residues in actin. In these assays, F-actin (5 μM) was added to either MBP–PfEMP3-F1a (5 μM) or MBP–Pf332-F19 (5 μM) before the other protein (titrated from 5.0 to 0.0 μM) was added and the mixture subsequently incubated. Resultant pellet and supernatant fractions were immunoblotted using either anti-MBP antiserum or monoclonal anti-actin antibodies. A. Constant concentrations of F-actin (5 μM) and MBP–PfEMP3-F1a (5 μM; ~60 kDa) were incubated with titrated serial dilutions of MBP–Pf332-F19 (5.0 to 0.0 μM; ~85 kDa) and centrifuged. No inhibition of MBP–PfEMP3-F1a binding to F-actin in the presence of increasing concentrations of MBP–Pf332-F19 (0.0 to 5.0 μM) was detected in the pelleted fractions. Only residual levels of the negative interaction control proteins MBP (5.0 μM), MBP–Pf332-F7 (5.0 μM), MBP–Pf332-F5 (5.0 μM) pelleted with F-actin. The positive interaction controls MBP–PfEMP3-F1a (5.0 μM) and MBP–Pf332-F19 (5.0 μM) each pelleting separately with F-actin were included. B. Constant concentrations of F-actin (5 μM) and MBP–Pf332-F19 (5 μM; ~85 kDa) were incubated with titrated serial dilutions of MBP–PfEMP3-F1a (5.0 to 0.0 μM; ~60 kDa) and centrifuged. No inhibition of MBP–Pf332-F19 binding to F-actin in the presence of increasing concentrations of MBP–PfEMP3-F1a (5.0 to 0.0 μM) was detected in the pelleted fractions. As above, only residual levels of the negative interaction control proteins MBP (5.0 μM), MBP–Pf332-F7 (5.0 μM), MBP–Pf332-F5 (5.0 μM) pelleted with F-actin. The positive interaction controls MBP–PfEMP3-F1a (5.0 μM) and MBP–Pf332-F19 (5.0 μM) each pelleting separately with F-actin were included.

compared to that of -F19, F19a and -F19c (Fig. 3B). Residues adjacent to defined binding regions that also contribute to overall interactions between RBC membrane skeleton and parasite proteins have been previously described for other *P. falciparum* proteins, including MESA and PfEMP3 [15,38]. Additionally, since comparatively more of the input -F19a protein remained in the insoluble fraction than -F19c (Fig. 3C), it is possible that -F19a may possess higher affinity for its binding partner in the RBC membrane skeleton than -F19c, but further experimentation would be required to confirm this suggestion. Further, calculation of the pI of actin and each MBP–Pf332 fusion protein (Table 1 and footnotes) indicates that it is unlikely that electrostatic forces are contributing significantly to any of the determined actin-binding affinities however, this phenomenon cannot be excluded for Pf332 binding to RBC membrane skeletons due to the heterogeneous nature of the proteins present in that binding substrate.

The moderate affinity half saturation concentrations (K_d) estimated for the 260 residue -F19 region binding to the RBC membrane skeleton or to purified actin are similar to those observed for other protein interactions that occur at the RBC membrane skeleton of uninfected or infected RBCs. In uninfected RBCs, the binding affinities of several protein interactions have been quantitated *in vitro*, including 4.1R binding to p55 ($K_{d(kin)} = 1 \times 10^{-7}$ M; [39]), protein 4.2 binding to band 3 ($K_d = 2\text{–}8 \times 10^{-7}$ M; [40]) and protein 4.2

binding to ankyrin ($K_d = 1–3.5 \times 10^{-7}$ M; [40]). These moderate affinities are also typical of those seen for malaria proteins binding at the membrane skeleton to host or malaria proteins *in vitro*. These include MESA binding to 4.1R ($K_{d(kin)} = 1.3 \times 10^{-7}$ M; [14]), KAHRP binding to PfEMP1 ($K_{d(kin)} = 1 \times 10^{-7}$ M; [22] and PfEMP3 binding to spectrin ($K_{d(kin)} = 3.8 \times 10^{-7}$ M; [15]). The similarity between the values determined for interactions between Pf332 and the membrane skeleton or purified actin is consistent with the proposition that actin may be the only protein at the IRBC membrane skeleton with significant ability to bind Pf332. We certainly cannot find any evidence for interaction of Pf332 with spectrin, but of course interaction assays using other purified native or recombinant RBC membrane skeleton proteins would be required to definitively exclude other partners. Although we cannot definitively exclude the possibility that the actin-binding affinity determined herein (using muscle actin) may be different to that derived using RBC actin, we believe that any differences are most likely to be subtle at best given the concordance between the Pf332 binding affinities estimated for RBC membrane skeletons ($K_d = 0.40$ μM) and actin ($K_d = 0.60$ μM).

In a previous study, we identified a 14 residue region of the parasite protein PfEMP3 that binds to both spectrin and actin [15]. Here, we used inhibition co-sedimentation assays to investigate whether the 260 residue actin-binding region of Pf332 was able to bind the same region in actin as PfEMP3. In these assays, F-actin was pre-incubated with either MBP–PfEMP3-F1a (which possesses the 14 residue actin-binding region) or MBP–Pf332-F19 before the addition of the other protein in a serially titrated fashion. Regardless of which protein was pre-incubated with F-actin, in each case the titrated protein was not able to discernibly inhibit the interaction of the pre-incubated protein with F-actin. Thus, from these experiments we were able to conclude that the proteins PfEMP3 and Pf332 most likely bind to physically separate residues in actin.

Pf322 has recently been implicated in both decreasing RBC membrane rigidity and in assisting trafficking of PfEMP1 to the IRBC membrane surface [31,32]. These studies showed that sequences located in the N-terminal region of Pf332 were important for adhesion and PfEMP1 trafficking, whereas sequences in the C-terminal domain of Pf332 were important in altered membrane rigidity [31]. The region we have identified as the Pf332 actin-binding region (residues 5115–5201) is deleted from these C-terminally truncated Pf332 mutant parasites. Together these data suggest that binding of Pf332 to membrane skeleton actin is required for modulating the structural and mechanical properties of the RBC membrane skeleton. In a normal membrane skeleton, interactions between αβ-spectrin heterodimers, actin and 4.1R facilitate the formation of a flexible lattice-like skeleton that is able to withstand repeated deformation in the microvasculature. Both 4.1R and actin bind to spectrin via sequences in the N-terminal 301 residue region of β-spectrin which encompasses the calponin homology domains (CH1 and CH2) [41]. Each of the CH1 and CH2 domains possess an actin and a 4.1R binding site. Thus, given that actin interacts with spectrin, and that the binding of 4.1R potentiates the interaction between spectrin and actin [42,43], it is likely that the binding of Pf332 to actin reduces actin's binding affinity for spectrin and 4.1R, resulting in suppression of membrane rigidity in the IRBC membrane skeleton. Additionally, binding of Pf332 to actin may also modulate actin's interactions with other membrane skeleton proteins including tropomyosin [44], adducin [45] and protein 4.9 (dematin) [46], however, further binding studies using purified native or recombinant RBC membrane skeleton proteins would be required to fully define these possible interactions and their effects on the membrane skeleton. The continued investigation of Pf332's interactions and the interactions of other parasite proteins at the IRBC membrane skeleton will ultimately expand our understanding of parasite-induced modifications that contribute significantly to the severe pathophysiology of *P. falciparum* malaria.

Acknowledgements

We thank Dr. Klavs Berzins for providing anti-Pf332 antiserum. This research was supported by grants and fellowships from the NHMRC (Howard Florey Centenary Research Fellowship to KLW; Senior Research Fellowship to BMC) and the NIH (grant #DK32094). We thank Kate Fernandez for expert technical assistance.

References

[1] R.W. Snow, C.A. Guerra, A.M. Noor, H.Y. Myint, S.I. Hay, The global distribution of clinical episodes of Plasmodium falciparum malaria, Nature 434 (2005) 214–217.
[2] B.M. Cooke, N. Mohandas, R.L. Coppel, Malaria and the red blood cell membrane, Semin. Hematol. 41 (2004) 173–188.
[3] L. Walensky, M. Narla, S. Lux IV, Disorders of the red blood cell membrane, in: R. Handin, S. Lux IV, T.P. Stossel (Eds.), Blood: Principles and Practice of Hematology, Lippincott, William and Wilkins, Philadelphia, 2003, pp. 1709–1858.
[4] P. Gascard, N. Mohandas, New insights into functions of erythroid proteins in nonerythroid cells, Curr. Opin. Hematol. 7 (2000) 123–129.
[5] A.M. Karinch, W.E. Zimmer, S.R. Goodman, The identification and sequence of the actin-binding domain of human red blood cell β-spectrin, J. Biol. Chem. 265 (1990) 11833–11840.
[6] P.O. Schischmanoff, R. Winardi, D.E. Discher, M.K. Parra, S.E. Bicknese, H.E. Witkowska, J.G. Conboy, N. Mohandas, Defining of the minimal domain of protein 4.1 involved in spectrin- actin binding, J. Biol. Chem. 270 (1995) 21243–21250.
[7] S.E. Lux, J. Palek, Disorders of the red cell membrane, in: R.I. Handin, S.E. Lux, T.P. Stossel (Eds.), Blood: Principles and Practice of Hematology, JB Lippincott Co., Philidelphia, 1995, pp. 1701–1818.
[8] M. Salomao, X. Zhang, Y. Yang, S. Lee, J.H. Hartwig, J.A. Chasis, N. Mohandas, X. An, Protein 4.1R-dependent multiprotein complex: new insights into the structural organization of the red blood cell membrane, Proc. Natl. Acad. Sci. U. S. A. 105 (2008) 8026–8031.
[9] M. Foley, L. Corcoran, L. Tilley, R. Anders, Plasmodium falciparum: mapping the membrane-binding domain in the ring-infected erythrocyte surface antigen, Exp. Parasitol. 79 (1994) 340–350.
[10] X. Pei, X. Guo, R. Coppel, S. Bhattacharjee, K. Haldar, W. Gratzer, N. Mohandas, X. An, The ring-infected erythrocyte surface antigen (RESA) of Plasmodium falciparum stabilizes spectrin tetramers and suppresses further invasion, Blood 110 (2007) 1036–1042.
[11] E. Da Silva, M. Foley, A.R. Dluzewski, L.J. Murray, R.F. Anders, L. Tilley, The Plasmodium falciparum protein RESA interacts with the erythrocyte cytoskeleton and modifies erythrocyte thermal stability, Mol. Biochem. Parasitol. 66 (1994) 59–69.
[12] M.D. Silva, B.M. Cooke, M. Guillotte, D.W. Buckingham, J.P. Sauzet, C. Le Scanf, H. Contamin, P. David, O. Mercereau-Puijalon, S. Bonnefoy, A role for the Plasmodium falciparum RESA protein in resistance against heat shock demonstrated using gene disruption, Mol. Microbiol. 56 (2005) 990–1003.
[13] B.J. Bennett, N. Mohandas, R.L. Coppel, Defining the minimal domain of the *Plasmodium falciparum* protein MESA involved in the interaction with the red cell membrane skeletal protein 4.1, J. Biol. Chem. 272 (1997) 15299–15306.
[14] K.L. Waller, W. Nunomura, X. An, B.M. Cooke, N. Mohandas, R.L. Coppel, Mature parasite-infected erythrocyte surface antigen (MESA) of Plasmodium falciparum binds to the 30-kDa domain of protein 4.1 in malaria-infected red blood cells, Blood 102 (2003) 1911–1914.
[15] K.L. Waller, L.M. Stubberfield, V. Dubljevic, W. Nunomura, X. An, A.J. Mason, N. Mohandas, B.M. Cooke, R.L. Coppel, Interactions of Plasmodium falciparum erythrocyte membrane protein 3 with the red blood cell membrane skeleton, Biochim. Biophys. Acta 1768 (2007) 2145–2156.
[16] X. Pei, X. Guo, R. Coppel, N. Mohandas, X. An, Plasmodium falciparum erythrocyte membrane protein 3 (PfEMP3) destabilizes erythrocyte membrane skeleton, J. Biol. Chem. 282 (2007) 26754–26758.
[17] B. Crabb, B.M. Cooke, J.C. Reeder, R.F. Waller, S.R. Caruana, K.M. Davern, M.E. Wickham, G.V. Brown, R.L. Coppel, A.F. Cowman, Targeted gene disruption shows that knobs enable malaria-infected red cells to cytoadhere under physiological shear stress, Cell 89 (1997) 287–296.
[18] M. Rug, S.W. Prescott, K.M. Fernandez, B.M. Cooke, A.F. Cowman, The role of KAHRP domains in knob formation and cytoadherence of P falciparum-infected human erythrocytes, Blood 108 (2006) 370–378.
[19] A. Kilejian, M.A. Rashid, M. Aikawa, T. Aji, Y.F. Yang, Selective association of a fragment of the knob protein with spectrin, actin and the red cell membrane, Mol. Biochem. Parasitol. 44 (1991) 175–182.
[20] C. Magowan, W. Nunomura, K.L. Waller, J. Yeung, J. Liang, H. Van Dort, P.S. Low, R.L. Coppel, N. Mohandas, Plasmodium falciparum histidine-rich protein 1 associates with the band 3 binding domain of ankyrin in the infected red cell membrane, Biochim. Biophys. Acta 1502 (2000) 461–470.
[21] X. Pei, X. An, X. Guo, M. Tarnawski, R. Coppel, N. Mohandas, Structural and functional studies of interaction between Plasmodium falciparum knob-associated histidine-rich protein (KAHRP) and erythrocyte spectrin, J. Biol. Chem. 280 (2005) 31166–31171.
[22] K.L. Waller, B.M. Cooke, W. Nunomura, N. Mohandas, R.L. Coppel, Mapping the binding domains involved in the interaction between the *Plasmodium falciparum* knob-associated histidine-rich protein (KAHRP) and the cytoadherence ligand

P. falciparum erythrocyte membrane protein 1 (PfEMP1), J. Biol. Chem. 274 (1999) 23808–23813.
[23] K.L. Waller, W. Nunomura, B.M. Cooke, N. Mohandas, R.L. Coppel, Mapping the domains of the cytoadherence ligand Plasmodium falciparum erythrocyte membrane protein 1 (PfEMP1) that bind to the knob- associated histidine-rich protein (KAHRP), Mol. Biochem. Parasitol. 119 (2002) 125–129.
[24] S.S. Oh, S. Voigt, D. Fisher, S.J. Yi, P.J. LeRoy, L.H. Derick, S. Liu, A.H. Chishti, Plasmodium falciparum erythrocyte membrane protein 1 is anchored to the actin-spectrin junction and knob-associated histidine-rich protein in the erythrocyte skeleton, Mol. Biochem. Parasitol. 108 (2000) 237–247.
[25] D. Mattei, A. Scherf, The *Pf332* gene of *Plasmodium falciparum* codes for a giant protein that is translocated from the parasite to the membrane of infected erythrocytes, Gene 110 (1992) 71–79.
[26] K. Hinterberg, A. Scherf, J. Gysin, T. Toyoshima, M. Aikawa, J.C. Mazie, L.P. da Silva, D. Mattei, *Plasmodium falciparum*: the Pf332 antigen is secreted from the parasite by a brefeldin A-dependent pathway and is translocated to the erythrocyte membrane via the Maurer's clefts, Exp. Parasitol. 79 (1994) 279–291.
[27] D. Mattei, A. Scherf, The Pf332 gene codes for a megadalton protein of Plasmodium falciparum asexual blood stages, Mem. Inst. Oswaldo Cruz 87 (1992) 163–168.
[28] N.L. Hiller, S. Bhattacharjee, C. van Ooij, K. Liolios, T. Harrison, C. Lopez-Estrano, K. Haldar, A host-targeting signal in virulence proteins reveals a secretome in malarial infection, Science 306 (2004) 1934–1937.
[29] M. Marti, R.T. Good, M. Rug, E. Knuepfer, A.F. Cowman, Targeting malaria virulence and remodeling proteins to the host erythrocyte, Science 306 (2004) 1930–1933.
[30] K. Moll, A. Chene, U. Ribacke, O. Kaneko, S. Nilsson, G. Winter, M. Haeggstrom, W. Pan, K. Berzins, M. Wahlgren, Q. Chen, A novel DBL-domain of the P. falciparum 332 molecule possibly involved in erythrocyte adhesion, PLoS ONE 2 (2007) e477.
[31] F.K. Glenister, K.M. Fernandez, L.M. Kats, E. Hanssen, N. Mohandas, R.L. Coppel, B.M. Cooke, Functional alteration of red blood cells by a megadalton protein of Plasmodium falciparum, Blood 113 (2009) 919–928.
[32] A.G. Maier, B.M. Cooke, A.F. Cowman, L. Tilley, Malaria parasite proteins that remodel the host erythrocyte, Nat. Rev. Microbiol. 7 (2009) 341–354.
[33] B.J. Morahan, G.B. Sallmann, R. Huestis, V. Dubljevic, K.L. Waller, Plasmodium falciparum: genetic and immunogenic characterisation of the rhoptry neck protein PfRON4, Exp. Parasitol. 122 (2009) 280–288.
[34] M.J. Gardner, H. Tettelin, D.J. Carucci, L.M. Cummings, L. Aravind, E.V. Koonin, S. Shallom, T. Mason, K. Yu, C. Fujii, J. Pederson, K. Shen, J. Jing, C. Aston, Z. Lai, D.C. Schwartz, M. Pertea, S. Salzberg, L. Zhou, G.G. Sutton, R. Clayton, O. White, H.O. Smith, C.M. Fraser, M.D. Adams, J.C. Venter, S.L. Hoffman, Chromosome 2 sequence of the human malaria parasite Plasmodium falciparum, Science 282 (1998) 1126–1132.
[35] A.R. Dluzewski, I.T. Ling, K. Rangachari, P.A. Bates, R.J. Wilson, A simple method for isolating viable mature parasites of Plasmodium falciparum from cultures, Trans. R. Soc. Trop. Med. Hyg. 78 (1984) 622–624.
[36] J. Wiesner, D. Mattei, A. Scherf, M. Lanzer, Biology of giant proteins of plasmodium: resolution of polyacrylamide-agarose composite gels, Parasitol. Today 14 (1998) 38–40.
[37] R.J. Howard, J.W. Barnwell, Roles of surface antigens on malaria-infected red blood cells in evasion of immunity, Contemp. Top. Immunobiol. 12 (1984) 127–200.
[38] J.F.J. Kun, K.L. Waller, R.L. Coppel, *Plasmodium falciparum*: structural and functional domains of the mature-parasite-infected erythrocyte surface antigen, Exp. Parasitol. 91 (1999) 258–267.
[39] W. Nunomura, Y. Takakuwa, M. Parra, J. Conboy, N. Mohandas, Regulation of protein 4.1R, p55, and glycophorin C ternary complex in human erythrocyte membrane, J. Biol. Chem. 275 (2000) 24540–24546.
[40] C. Korsgren, C.M. Cohen, Associations of human erythrocyte band 4.2. Binding to ankyrin and to the cytoplasmic domain of band 3, J. Biol. Chem. 263 (1988) 10212–12028.
[41] X. An, G. Debnath, X. Guo, S. Liu, S.E. Lux, A. Baines, W. Gratzer, N. Mohandas, Identification and functional characterization of protein 4.1R and actin-binding sites in erythrocyte beta spectrin: regulation of the interactions by phosphatidy-linositol-4, 5-bisphosphate, Biochemistry 44 (2005) 10681–10688.
[42] C.M. Cohen, S.F. Foley, Biochemical characterization of complex formation by human erythrocyte spectrin, protein 4.1, and actin, Biochemistry 23 (1984) 6091–6098.
[43] V. Ohanian, L.C. Wolfe, K.M. John, J.C. Pinder, S.E. Lux, W.B. Gratzer, Analysis of the ternary interaction of the red cell membrane skeletal proteins spectrin, actin, and 4.1, Biochemistry 23 (1984) 4416–4420.
[44] V.M. Fowler, V. Bennett, Erythrocyte membrane tropomyosin. Purification and properties, J. Biol. Chem. 259 (1984) 5978–5989.
[45] K. Gardner, V. Bennett, Modulation of spectrin-actin assembly by erythrocyte adducin, Nature 328 (1987) 359–362.
[46] A. Husain-Chishti, A. Levin, D. Branton, Abolition of actin-bundling by phosphor-ylation of human erythrocyte protein 4.9, Nature 334 (1988) 718–721.
[47] R.L. Coppel, K.M. Davern, M.J. McConville, Immunochemistry of parasite antigens, in: C.J. van Oss, M.H.V. van Regenmortel (Eds.), Immunochemistry, Marcel Dekker, Inc, New York, 1994, pp. 475–531.